Accepted Manuscript

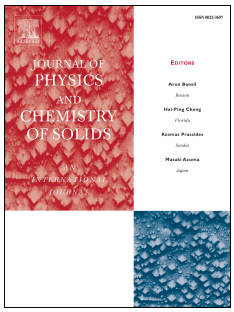

Thermodynamics of the melting process in Au nano-clusters: Phenomenology, energy, entropy and quasi-chemical modeling

Dalía S. Bertoldi, Emmanuel N. Millán, Armando Fernández Guillermet

PII: S0022-3697(17)30848-X

DOI: 10.1016/j.jpcs.2017.08.010

Reference: PCS 8164

To appear in: *Journal of Physics and Chemistry of Solids*

Received Date: 15 May 2017

Revised Date: 0022-3697 0022-3697

Accepted Date: 3 August 2017

Please cite this article as: Dalí.S. Bertoldi, E.N. Millán, Armando.Ferná. Guillermet, Thermodynamics of the melting process in Au nano-clusters: Phenomenology, energy, entropy and quasi-chemical modeling, *Journal of Physics and Chemistry of Solids* (2017), doi: 10.1016/j.jpcs.2017.08.010.

Thermodynamics of the melting process in Au nano-clusters: phenomenology, energy, entropy and quasi-chemical modeling †

Dalía S. Bertoldi[a,*], Emmanuel N. Millán[b], Armando Fernández Guillermet[c]

[a] *Instituto de Investigación y Desarrollo en Ingeniería de Procesos, Biotecnología y Energías Alternativas CONICET - UNCo, Neuquén, Argentina*
[b] *Facultad de Ciencias Exactas y Naturales - Universidad Nacional de Cuyo, Mendoza, Argentina*
[c] *CONICET - Instituto Balseiro, Centro Atómico Bariloche, Argentina*

Abstract

The paper presents a thermodynamic study of the melting transition in Au nano-clusters with a number of atoms (N) in the range $10^3 < N < 10^6$ using a Molecular Dynamics (MD) technique. This range of sizes allows an analysis of the relations between the properties of the clusters and macroscopic Au. Four steps in the progress of the transition occurring upon heating are identified on thermodynamic and structural basis, and the corresponding temperature ranges are determined. In particular, the step where most of the transition takes place (the "melting step") is identified and described in terms of the change in the relative amount of two kinds of atoms, viz., those forming solid phase-like (SPL) aggregates and those in the liquid phase-like (LPL) aggregates. The energy and entropy change involved in the "melting step" are established as a function of N. These properties are used to evaluate the temperature T_0 at which the SPL and the LPL have equal values of the Helmholtz energy. Furthermore, the possibility of describing the thermodynamics of the "melting step" by means of a formalism involving an isomerization-type reaction between the atoms in the SPL and the LPL is explored. To this aim, an equilibrium constant (K_{eq}) involving the concentration of such types of atoms is introduced. Finally, it is shown that a thermodynamic, van't Hoff analysis of the size-dependence of K_{eq} yields values of the T_0 temperature which are in very good agreement with those obtained from the energy and entropy values.

Keywords: A. Nanostructures, A. Metals, C. Molecular Dynamics, D. Phase transitions, D.Thermodynamic properties

1. Introduction

The study of the melting transition constitutes a long-standing tradition in the fields of physics and chemistry of elemental nano-clusters (early works in this field are quoted,

*I am corresponding author
Email address: daliasurena_ber@hotmail.com (Dalía S. Bertoldi)

for example, in refs. [1, 2, 3] and references in there). Among the classical research issues, the question of the effect of cluster size upon the melting process has recently received a considerable attention. A significant part of the experimental and analytical work has focused on the characterization of the temperature at which the process takes place [4, 5, 6, 7, 8]. Moreover, by using Molecular Dynamics (MD) simulations it has been possible to determine the energy versus temperature, i.e., the so-called "caloric" curves for nano-clusters [9, 10, 11, 12, 13, 14, 15].

A striking result of the MD work on elements is the fact that the melting transition of nano-clusters occurs in a finite temperature range, contradicting what is expected from Gibbs' Phase Rule for macroscopic, elemental matter at constant pressure, viz., a unique melting temperature [16, 17, 18, 19]. This finding calls into question the adoption of a single melting temperature for nano-clusters in discussions of, i.a., the size dependence of the Debye temperature through Lindemann's empirical formula [20, 21, 22, 23]. This, of course, does not preclude the use of indices inspired in the Lindemann picture of the melting phenomenon as useful tools to characterize the onset and the progress of the transition [9, 11].

The general purpose of the present study is to perform a theoretical thermodynamic characterization of the melting process in Au nano-clusters, using MD simulations. In the following we summarize the specific motivations and the outline of the paper.

In the first place, Au has been chosen because its various technological and biomedical applications [24, 25, 26], as testified by numerous experimental and theoretical studies [4, 27, 28, 29]. Secondly, as a difference with the traditional interest on small (10-500 atoms [3, 10, 30]) or medium-size (500-5000 atoms [10, 31, 32]) clusters the current work aims at establishing thermodynamic trends in a range of sizes which allows a meaningful comparison with the properties of the macroscopic material. To this aim spherical nano-clusters with $10^3 - 10^6$ atoms of Au are studied.

In the first part of the paper, the onset and progress of the melting process is established by a combined methodology involving the analysis of the caloric curves, as well as the use of various structure-sensitive parameters, viz., a previously suggested Lindemann index [9, 11, 15, 33], the temperature and radial dependence of the root-mean square displacement and the radial distribution function. On these bases, a phenomenological description of the process occurring upon heating is presented, which involve the transition between two "phase-like" aggregates of atoms, corresponding to what in macroscopic thermodynamics is called the solid and the liquid phase, respectively. By considering thermodynamic and structural information, a four-step description of the process is developed. In particular, the step where the major part of the transition takes place (referred to in the work as the "melting step") is identified. The "melting step" is described microscopically in terms of the continuous variation with temperature of the relative amounts of two kinds of atoms, viz., the low-energy atoms forming solid phase-like (SPL) aggregates, and the high-energy atoms forming liquid phase-like (LPL) aggregates. A key element of the work is the determination of the characteristic energy of these types of atoms by analyzing the caloric curves (see below).

In the second part of the paper, the thermodynamic implications of this qualitative description of the "melting step" are explored in two ways. First, the energy and entropy

involved are determined by analyzing the caloric curves obtained by MD. With these values, the temperature at which the SPL and the LPL aggregates have the same Helmholtz energy (usually referred to as the T_0 temperature) is determined as a function of N. Second, the change upon heating of the relative amounts of the atoms in the SPL and LPL aggregates in the "melting step" is modeled as the variations in concentration of a "two-component" system which is undergoing an isomerization-like reaction. Specifically, relying upon previous ideas by Berry [34, 35, 18, 19] a thermodynamic "equilibrium constant" for such a reaction will be defined and evaluated for the present nano-clusters. Third, it is shown that the formalism of the equilibrium constant also leads to predictions of the T_0 temperature, which are to be compared with those obtained from the energy and entropy values extracted from the caloric curve.

2. Theoretical method

Au nano-clusters with 1985-1010079 atoms were created with the LAMMPS code [36] as spheres of different radius centered at the origin of the fcc lattice. It has been argued that this spherical geometry can stably exist in nature[37]. The clusters were treated by adopting an EAM interaction potential, as extensively used in previous works to study the melting of Au nano-clusters[3, 31, 32, 27].

The current clusters have a free-surface boundary condition at given temperatures under zero external pressure. The temperature was increased in steps of 10-50 K (50 K only at low temperatures) in 200 ps (with a time-step of 0.001 ps) until the melting occurred. At each temperature, another MD run of 200 ps was made: the first 100 ps were used for equilibration and the following 100 ps to obtain statistical data. For sizes larger than 37000 atoms, steps of 5 K near the melting range were adopted, whereas steps of 2 K were used with the cluster with $N = 1010079$. In order to start with the most stable cluster configuration, an energy minimization procedure was applied at the start of the MD runs. A similar heating process has been used in ref. [10]

3. Thermal and microscopic characterization of the melting process

3.1. Methodology

The onset and progress of the melting process was studied by combining the analysis of the MD caloric curves (as discussed below) with a consideration of the following parameters describing the structure and dynamics of the nano-cluster:

1. The cluster Lindemann index (δ_c), obtained as the average of the indices for each atom (δ_i), calculated in turn as a function of temperature as follows [9, 11]:

$$\delta_i = \frac{1}{N-1} \sum_{j(\neq i)} \frac{\sqrt{\langle r_{ij}^2 \rangle_T - \langle r_{ij} \rangle_T^2}}{\langle r_{ij} \rangle_T} \tag{1}$$

In Eq. (1) N is the number of atoms in the cluster, $\langle ... \rangle$ denotes the thermal average at temperature T and r_{ij} is the distance between the i_{th} and j_{th} atoms. δ_c typically

has low values for solids and higher for liquids [33] which allows the identification of the "melting step".

2. The root-mean square displacement (RMSD), calculated as

$$RMSD = \left\langle \sqrt{\frac{1}{n}\sum_{i=1}^{n}(r_i(t) - r_i(0))^2} \right\rangle_T \quad (2)$$

In Eq.(2), $r_i(0)$ is the reference position of each particle, $r_i(t)$ the position at determined time t and n the number of atoms in different shells.
To follow the evolution of the atomic motions the cluster was partitioned into four radial shells with equal thickness (dr), allowing the RMSD to be determined in each shell. In this way, in addition to information on the changes in the interatomic distances (given by δ_i) the changes in the position of each atom (with respect to itself) were characterized in terms of the $RMSD$.

3. The radial distribution function $N(r)$ within each shell, defined as:

$$N(r) = 4\pi r^2 \rho dr \quad (3)$$

where ρ is the number density. This function characterizes the average structural environment of the atoms, reflecting the degree of order in the cluster. Thus, for any given cluster size, $N(r)$ gives information on the melting process.

4. Several snapshots of the clusters' sections at various temperatures, which were used to visualize the melting process.

3.2. Radial and size dependence

The caloric curves (square symbols) and cluster Lindemann indices (δ_c) (circles) obtained for nano-clusters of three of the studied sizes are presented in Fig 1. In the figure we also include the incremental ratio of these two quantities (open symbols). Fig. 2 presents snapshots of the clusters sections at several temperatures. The atoms that at the beginning of the heating were located at the surface, are painted in red.

On the basis of this information, the progress upon heating of the melting process will be described in terms of four steps, with the respective temperature ranges indicated with the vertical lines (dashed in Fig.1 and dotted in Fig.2), as follows:

1. The first step corresponds to materials in the SPL state: in this temperature range, the atoms are found in their crystalline positions (see the first column in Fig.2).
2. At about 800 K the plots of the caloric curves and the Lindemann index (Fig. 1) show increases in slope, which will be interpreted as the onset of a new step, referred to in the following as "pre-melting step". Here the surface atoms start to move, occupying the position of their neighbors, i.e., a diffusion process occurs (Fig 2, second column).
3. Between the second and third dotted lines, the plots of the caloric curves and the δ_c parameters show a drastic increase with temperature, determining what we will call the "melting step". Here the diffusion involves even the inner atoms (see Fig.2, third

column). As found in [9, 10], in this temperature range, SPL and LPL aggregates coexist in comparable proportions. The "melting step" of the caloric curve, tends to become vertical when the cluster size approaches the macroscopic limit.

4. Finally, at the fourth step, clusters are found in a LPL state: the painted atoms originally located at the surface are found anywhere in the cluster (Fig. 2, fourth column). It should be remarked that the quantity E/N in this state also differs for different sizes because the clusters are quasi-spherical after melting, so that the LPL state also has a "surface".

This description is phenomenological and is based in the behavior of the parameters shown in Fig. 1. The fractions of the atoms in the states SPL and LPL will be presented in Section 5.

In order to analyze the effect of temperature upon the atomic motions, the RMSD (Eq. 2) and the $N(r)$ (Eq. 3) functions were studied as a function of the distance from the center of the cluster. To this end, we partitioned the clusters into five shells and evaluated RMSD and $N(r)$ in each one. The so-obtained RMSD were then compared with the inter-atomic distance d of Au (viz., $d = 2.9\dot{A}$). The resulting $RMSD/d$ ratios for clusters with N=1985, 15705 and 180313 and various temperatures are plotted in Fig.3(a), 3(b) and 3(c), respectively, versus the distance from the each shell to the center of the nano-cluster. The horizontal dashed line indicates value $RMSD/d = 1$, adopted here as a reference level.

At low temperatures the RMSD is close to zero and the atoms are arranged in an fcc crystal lattice. At higher temperatures, the $RMSD$ of the outermost shell is larger than those for the inner shells, suggesting that the surface of the nano-cluster is in a LPL state whereas the inner shells are still in the SPL state. As the temperature reaches 970 K (Fig.3(a)), 1060 K (Fig.3(b)) and 1095 K (Fig.3(c)), the $RMSD$ of the shells exceeds the interatomic distance, and the cluster suddenly transforms to LPL state. It should be emphasized that a similar behavior has been reported for clusters of V[12] and Cu [13].

This behavior is also reflected in Figure 4 where $N(r)$ for the innermost and outermost shells are shown. In this figure we included only the results corresponding to N=15705 (upper panel) and N=180313 (lower panel) because the cluster with N=1985 is too small to allow a calculation of the number density over regions. The arrows in these plots are used to mark some relevant differences in the patterns of $N(r)$ at the same temperature. At 400 K both sizes show $N(r)$ functions with sharp and well defined peaks in all shells, which is characteristic of a crystalline structure. At higher temperatures, the core of the cluster exhibits sharp peaks whereas the only peak that remains clearly distinguishable in the surface is the one corresponding to the smallest inter-atomic distance ($r_{Au-Au} = d$). At temperatures where $RMSD/d > 1$, $N(r)$ has the shape characteristic of a liquid phase [38].

4. Energy and entropy of melting

4.1. Methodology

Once the temperature ranges corresponding to the "melting step" (Fig.1 and 2) of the clusters have been identified, the corresponding energy changes ($\Delta E_m(N)$) were determined from the caloric curves as a function of N.

Next, the entropy of melting of each clusters ($\Delta S_m(N)$) was evaluated from $\Delta E_m(N)$ by using the following thermodynamic formula, obtained by integrating by parts the identity $dS = dE/T$ between the temperatures T_{II} and T_{III} corresponding, respectively, to the lowest and highest temperature limits of the "melting step" (see Figs. 1 and 2):

$$\Delta S_m(N) = \frac{E_{III}}{T_{III}} - \frac{E_{II}}{T_{II}} + \int_{T_{II}}^{T_{III}} \frac{E}{T^2} dT \qquad (4)$$

4.2. Size dependence

The $\Delta E_m(N)$ vs. $N^{-1/3}$ relations obtained in the present work are shown in Fig. 5 (a). The energy change associated to the "melting step" decreases with the size of the cluster. In particular, a linear variation with $N^{-1/3}$ is found, which is consistent with the predictions of previously reported models and simulations of metallic clusters [39, 40, 41].

It should be remarked that macroscopic Au is not dealt within the current work, because: (i) its properties are well established experimentally and using the EAM potential, and (ii) it is known that the MD simulation of the melting of bulk crystals poses various problems. In particular, the use of periodic boundary conditions has been reported to lead to overheating up to temperatures much higher than the equilibrium melting point [42]. A frequent solution to this is to increase the size of the simulated sample, but this in turn involves large demands of computational capacity. Another solution is to introduce an interface as a starting configuration and study its equilibrium [42]. However this situation is physically different to that adopted here to study the melting of nano-clusters.

In view of these problems, an alternative route to estimate the energy change corresponding to the macroscopic "melting step" was adopted in the current work, viz., the ΔE^{bulk} value was obtained by a linear extrapolation of the current $\Delta E_m(N)$ vs. $N^{-1/3}$ results, as indicated by the dashed line in Fig. 5. In this way we obtained $\Delta E^{bulk} = (9.9 \pm 0.1)$ KJ/mol. As usually found in MD simulations using the EAM potential [31], this value differs from the experimental ΔE^{bulk} viz., 12.4 KJ/mol. Also in accord with the general trends, the current ΔE^{bulk} compares very well with the value 10.6 KJ/mol obtained in a previously reported EAM simulation [31].

The $\Delta S_m(N)$ vs. $N^{-1/3}$ values obtained by applying Eq.(4) are plotted in Fig. 5 (b). The value for ΔS^{bulk} was calculated as the ratio between the estimated ΔE^{bulk} and a melting temperature T_m for macroscopic Au which is discussed in Sect. 5. In this way we obtained $\Delta S^{bulk} = (8.9 \pm 0.1)$ J/mol K. As expected, ΔS^{bulk} differs from the experimental entropy of melting (viz., 9.6 J/mol K [43]). No entropy of melting values for Au nano-clusters have been found in the literature to compare with the current results.

Figure 5 (b) indicates that $\Delta S_m(N)$ also depends linearly upon with $N^{-1/3}$. This trend is qualitatively consistent with the predictions of previously reported models for nanoparticles [39, 40, 41]. By relying upon the linear dependence, a value of ΔS^{bulk} might also be obtained by extrapolation. Such procedure yields $\Delta S^{bulk} = 9.2 \pm 0.1$, which agrees well with the ΔS^{bulk} value listed above (see Section 5).

Trends in Fig. 5 show that the energy needed to pass from SPL state to LPL state is lower for small clusters. This suggests that the structural difference between the two states

decreases with cluster size. In view of this fact, it is not surprising that ΔS also decreases with size. Indeed, both ΔE and ΔS vary linearly with $N^{-1/3}$, i.e. the $surface/volume$ ratio, as found in other structural and cohesive properties of clusters [44].

4.3. Thermodynamic consequences

Since the melting process of the nano-clusters occurs in a temperature range, it is not possible to determine a unique "melting temperature". Therefore, the size dependence of the "melting step" will be characterized in terms of temperature T_0, which represents, in macroscopic thermodynamics, a temperature such that the Helmholtz energy ($F = E - TS$) of two phases is the same. The T_0 temperature is traditionally adopted in thermodynamic analyses of e.g., the martensitic transformation in macroscopic alloys, to connect the treat the experimental phase transition temperatures with the thermodynamic properties of the phases involved [45, 46, 47]. In the current work, T_0 of the transition between the SPL and LPL of Au nano-clusters, becomes the temperature at which:

$$F^{LPL} = E^{LPL} - T_0 S^{LPL} = E^{SPL} - T_0 S^{SPL} = F^{SPL} \tag{5}$$

Solving Eq.(5) for a nano-cluster with N atoms yields:

$$T_0(N) = \frac{E^{LPL} - E^{SPL}}{S^{LPL} - S^{SPL}} = \frac{\Delta E_m(N)}{\Delta S_m(N)} \tag{6}$$

The T_0 versus $N^{-1/3}$ relation obtained by inserting in Eq.(6) the results of the current simulations is presented in Fig. 8 using solid squares. A well-defined linear variation is found (dashed line), which would allow a reasonably accurate least-squares extrapolation to the macroscopic limit. The extrapolated value is particularly important in the present analysis because, by definition, it corresponds to the temperature of the "melting step" of macroscopic Au, since:

$$\lim_{N\to\infty} T_0(N) = \lim_{N\to\infty} \frac{\Delta E_m(N)}{\Delta S_m(N)} = \frac{\Delta E_m^{bulk}}{\Delta S_m^{bulk}} = T_m \tag{7}$$

5. Quasi-chemical modeling of the "melting step"

The "melting step" in the current nano-clusters was qualitatively discussed in Section 2 in terms of the increase (decrease) upon heating, of the number of atoms in LPL (SPL) aggregates. Such an approach is comparable but, of course, not identical, to previous treatments of the melting transition based on "two-state" (or "two-level") energy models[48, 49, 50, 51]. In the following, the current qualitative ideas will be formalized, and related to the thermodynamic properties determined in the previous sections, as follows:

1. At each temperature in the range corresponding to the "melting step", the relative amounts of atoms in SPL and LPL will be expressed by adopting the usual concentration variables (X_j) of each kind of atoms. In the language of macroscopic solution thermodynamics, the X_j concentration of each component of this "binary system" is

established. The X_j values were determined as a function of T by analyzing the part of the caloric curves corresponding to the "melting step" and making use of the fact that energy is an extensive function. Then:

$$X_{LPL} = \frac{E_X - E_{II}}{\Delta E_m} \tag{8}$$

$$X_{SPL} = 1 - X_{STA} \tag{9}$$

In Eq.(8) E_X is a general energy value falling between the energy bounds of the "melting step", viz., the values E_{II} and E_{III}, indicated in Fig.6 on the caloric curve of a cluster with N=180313. The temperature dependence of the variables X_{SPL} and X_{LPL} determined by applying Eqs.(8) and (9) to the same nano-cluster is presented in Fig. 7.

2. The progress of the "melting step" upon heating will be described by the changes in the components' relative fractions caused by an isomerization-like reaction between Au atoms in SPL and LPL, respectively, viz.,

$$Au(SPL) \rightarrow Au(LPL) \tag{10}$$

3. At a given temperature within the "melting step" the equilibrium concentrations X_{SPL} and X_{LPL} will be connected by an equilibrium constant (K_{eq}) which depends both upon T and N. Such constant will be formulated as in macroscopic thermodynamics [1], i.e.,

$$K_{eq}(T, N) = \frac{X_{LPL}}{X_{SPL}} \tag{11}$$

4. Combination of the standard van't Hoff relation with Eq.(11) yields:

$$\Delta^0 F = -RT \ln K_{eq}(T, N) \tag{12}$$

where $\Delta^0 F$ represents the difference in Helmholtz energy between the pure "components", viz., SPL and LPL aggregates formed by N atoms pure Au at the temperature T. By evaluating Eq.(12) at the temperature T_0 introduced in Sect.4.3 yields, by definition:

$$K_{eq}(T_0, N) = 1 \tag{13}$$

$$X_{LPL}(T_0, N) = X_{SPL}(T_0, N) \tag{14}$$

5. Using Eq.(14) the T_0 temperature of the cluster with N=180313 was determined (Fig.7). The T_0 values obtained by applying this procedure to all current clusters (solid circles) and compared in Fig. 8 with those obtained by applying Eq. (6).

The possibility of a small systematic difference between the T_0 values obtained by these methods (Fig. 8) cannot be ruled out. However the discrepancy is hardly larger than the error bars. Therefore the general agreement shown by Fig. 8 is considered by us as an indirect indication of the plausibility of the current isomerization-reaction type modeling of the "melting step".

In particular, a linear extrapolation of the results (following the dashed line) yields $T_m = (1113 \pm 7)\,\mathrm{K}$ for the melting point of macroscopic Au. A previously reported Monte Carlo study using EAM to determine the Gibbs energy of the bulk phases yielded 1090 K [52]. Another EAM study of the melting of clusters as a function of N [32] allows a similar extrapolation to $N^{-1/3} = 0$, which yields $(1128 \pm 13)\,\mathrm{K}$. The current value is almost exactly the average of these previous results.

6. Summary and concluding remarks

The purpose of the current work is to add to the understanding of the thermodynamics of the melting process occurring upon heating of spherical Au nano-clusters. A key ingredient of the work is the determination of the caloric curves using a Molecular Dynamics technique and the use of such results to determine the size dependence of energy and entropy change associated to what is referred to as the "melting step" of the process.

In agreement with previous studies, the work has established that such step in Au nano-clusters occurs in a temperature range, which contradicts the predictions of Gibbs' Phase Rule for a solid/liquid transition in a macroscopic unary system.

The conceptual strategy of the work involves, in the first place, a identification at the nano-scale of the "solid phase-like" and "liquid phase-like" structures involved in the "melting step". To this end, a microscopic criterion is introduced, which involves the energy of the atoms forming those "solid phase-like" and "liquid phase-like" aggregates, and exploring the thermodynamic consequences of such qualitative picture.

The current consideration of two kinds of atoms at the nano-scale might be thought of as the microscopic counterpart of considering a macroscopic system as a "two-component" one when applying the Phase Rule. These ideas, which have roots in the enlightening work by Stephen Berry are tested in detail in the current work by modeling the "melting step" of the process in terms of an isomerization-like reaction between two types of atoms.

An equilibrium constant involving the concentrations of these two "components" is introduced and used to predict the size dependence of the so-called "equal-Helmholtz energy temperature", T_0. The results are compared with a direct thermodynamic calculation of T_0 which makes use of the energy and entropy changes involved in the "melting step" that were extracted from the caloric curves. A reasonably good general agreement is found, which adds to the confidence on the thermodynamic consistency and the plausibility of the current approach.

Acknowledgment

This work was supported by Project PIP 112-20110100814 from CONICET and Project I197

from Universidad Nacional del Comahue. This work used the cluster Toko from Universidad Nacional de Cuyo, which is part of the SNCAD network.

[1] T. Hill, Thermodynamics of Small Systems, Dover Phoenix editions, Dover Publications, 1994.
[2] T. L. Beck, R. S. Berry, The interplay of structure and dynamics in the melting of small clusters, The Journal of Chemical Physics 88 (6) (1988) 3910–3922.
[3] C. Cleveland, W. Luedtke, U. Landman, Melting of gold clusters, Physical Review B 60 (7) (1999) 5065.
[4] G. Guenther, O. Guillon, Models of size-dependent nanoparticle melting tested on gold, Journal of Materials Science 49 (23) (2014) 7915–7932.
[5] M. Liu, R. Y. Wang, Size-dependent melting behavior of colloidal In, Sn, and Bi nanocrystals, Scientific reports 5 (2015) 16353.
[6] E.-H. Kim, B.-J. Lee, Size dependency of melting point of crystalline nano particles and nano wires: A thermodynamic modeling, Metals and Materials International 15 (4) (2009) 531–537.
[7] A. Chernyshev, Melting of surface layers of nanoparticles: Landau model, Materials Chemistry and Physics 112 (1) (2008) 226–229.
[8] G. Melnikov, S. Yemelianov, N. Ignatenko, E. Cherkasov, O. Manzhos, Cluster melting in effective potential model, in: IOP Conference Series: Materials Science and Engineering, Vol. 168, IOP Publishing, 2017, p. 012021.
[9] J. Jellinek, T. L. Beck, R. S. Berry, Solid–liquid phase changes in simulated isoenergetic Ar13, The Journal of Chemical Physics 84 (5) (1986) 2783–2794.
[10] J.-H. Shim, B.-J. Lee, Y. W. Cho, Thermal stability of unsupported gold nanoparticle: a Molecular Dynamics study, Surface science 512 (3) (2002) 262–268.
[11] H. Duan, F. Ding, A. Rosén, A. R. Harutyunyan, S. Curtarolo, K. Bolton, Size dependent melting mechanisms of iron nanoclusters, Chemical Physics 333 (1) (2007) 57–62.
[12] W. Hu, S. Xiao, J. Yang, Z. Zhang, Melting evolution and diffusion behavior of vanadium nanoparticles, The European Physical Journal B-Condensed Matter and Complex Systems 45 (4) (2005) 547–554.
[13] L. Wang, Y. Zhang, X. Bian, Y. Chen, Melting of cu nanoclusters by molecular dynamics simulation, Physics Letters A 310 (2) (2003) 197–202.
[14] H. Li, R. Xu, Z. Bi, X. Shen, K. Han, Melting properties of medium-sized silicon nanoclusters: A molecular dynamics study, Journal of Electronic Materials (2016) 1–5.
[15] I. Hamid, M. Fang, H. Duan, Molecular dynamical simulations of melting behaviors of metal clusters, AIP Advances 5 (4) (2015) 047129.
[16] R. S. Berry, When the melting and freezing points are not the same, Scientific American (August) (1990) 68–73.
[17] R. S. Berry, B. M. Smirnov, Two-state approximation for aggregate states of clusters, The Journal of Chemical Physics 114 (15) (2001) 6816–6823.
[18] R. S. Berry, B. M. Smirnov, Observability of coexisting phases of clusters, International Journal of Mass Spectrometry 280 (1) (2009) 204–208.
[19] R. S. Berry, B. M. Smirnov, Bridging the macro and micro, Chemical Physics Letters 573 (2013) 1–4.
[20] Q. Jiang, H. Tong, D. Hsu, K. Okuyama, F. Shi, Thermal stability of crystalline thin films, Thin Solid Films 312 (1) (1998) 357–361.
[21] Y. Zhu, J. Lian, Q. Jiang, Modeling of the melting point, Debye temperature, thermal expansion coefficient, and the specific heat of nanostructured materials, The Journal of Physical Chemistry C 113 (39) (2009) 16896–16900.
[22] J. Chandra, K. Kholiya, Diameter-dependent thermodynamic and elastic properties of metallic nanoparticles, Modern Physics Letters B 29 (08) (2015) 1550025.
[23] C. C. Yang, S. Li, Investigation of cohesive energy effects on size-dependent physical and chemical properties of nanocrystals, Physical Review B 75 (16) (2007) 165413.
[24] S. K. Ghosh, T. Pal, Interparticle coupling effect on the surface plasmon resonance of gold nanoparticles: from theory to applications, Chemical reviews 107 (11) (2007) 4797–4862.

[25] B. Hvolbæk, T. V. Janssens, B. S. Clausen, H. Falsig, C. H. Christensen, J. K. Nørskov, Catalytic activity of Au nanoparticles, Nano Today 2 (4) (2007) 14–18.
[26] I. H. El-Sayed, X. Huang, M. A. El-Sayed, et al., Surface plasmon resonance scattering and absorption of anti-EGFR antibody conjugated gold nanoparticles in cancer diagnostics: applications in oral cancer, Nano letters 5 (5) (2005) 829–834.
[27] S. Ali, V. Myasnichenko, E. Neyts, Size-dependent strain and surface energies of gold nanoclusters, Physical Chemistry Chemical Physics 18 (2) (2016) 792–800.
[28] Z. Qiao, H. Feng, J. Zhou, Molecular dynamics simulations on the melting of gold nanoparticles, Phase Transitions 87 (1) (2014) 59–70.
[29] N. Wang, S. Rokhlin, D. Farson, Nonhomogeneous surface premelting of Au nanoparticles, Nanotechnology 19 (41) (2008) 415701.
[30] L. Reinaudi, M. C. Giménez, Monte carlo simulation of gold and silver nanoparticles in interaction with strongly surfactant media, Journal of Computational and Theoretical Nanoscience 10 (10) (2013) 2507–2519.
[31] Y. G. Chushak, L. S. Bartell, Melting and freezing of gold nanoclusters, The Journal of Physical Chemistry B 105 (47) (2001) 11605–11614.
[32] L. J. Lewis, P. Jensen, J.-L. Barrat, Melting, freezing, and coalescence of gold nanoclusters, Physical Review B 56 (4) (1997) 2248.
[33] Y. Engelmann, A. Bogaerts, E. C. Neyts, Thermodynamics at the nanoscale: phase diagrams of nickel–carbon nanoclusters and equilibrium constants for phase transitions, Nanoscale 6 (20) (2014) 11981–11987.
[34] R. S. Berry, Phase transitions in clusters: a bridge to condensed matter, in: Linking the Gaseous and Condensed Phases of Matter: The Behavior of Slow Electrons, Springer, 1994, pp. 231–249.
[35] R. S. Berry, Phases and phase changes of clusters, in: Large Clusters of Atoms and Molecules, Kluwer Academic, 1996, pp. 281–295.
[36] S. Plimpton, Fast parallel algorithms for short-range Molecular Dynamics, Journal of Computational Physics 117 (1) (1995) 1–19.
[37] P. D. Jadzinsky, G. Calero, C. J. Ackerson, D. A. Bushnell, R. D. Kornberg, Structure of a thiol monolayer-protected gold nanoparticle at 1.1 å resolution, Science 318 (5849) (2007) 430–433.
[38] D. Tabor, Gases, Liquids and Solids: And Other States of Matter, Cambridge University Press, 1991.
[39] H. Omid, H. Delavari H, H. R. Madaah Hosseini, Melting enthalpy and entropy of freestanding metallic nanoparticles based on cohesive energy and average coordination number, The Journal of Physical Chemistry C 115 (35) (2011) 17310–17313.
[40] Y. Qi, T. Çağin, W. L. Johnson, W. A. Goddard III, Melting and crystallization in Ni nanoclusters: The mesoscale regime, The Journal of chemical physics 115 (1) (2001) 385–394.
[41] A. Safaei, M. A. Shandiz, Size-dependent thermal stability and the smallest nanocrystal, Physica E: Low-dimensional Systems and Nanostructures 41 (3) (2009) 359–364.
[42] A. B. Belonoshko, L. S. Dubrovinsky, Molecular dynamics of NaCl (B1 and B2) and MgO (B1) melting: Two-phase simulation, American Mineralogist 81 (3-4) (1996) 303–316.
[43] Z. Jian, K. Kuribayashi, W. Jie, Solid-liquid interface energy of metals at melting point and undercooled state., Materials Transactions 43 (4) (2002) 721–726.
[44] E. Roduner, Size matters: why nanomaterials are different, Chemical Society Reviews 35 (7) (2006) 583–592.
[45] S. Cotes, M. Sade, A. Fernández Guillermet, Fcc/hcp martensitic transformation in the Fe-Mn system: Experimental study and thermodynamic analysis of phase stability, Metallurgical and Materials Transactions A 26 (8) (1995) 1957–1969.
[46] A. Baruj, A. Fernández Guillermet, M. Sade, The fcc/hcp relative phase stability in the Fe-Mn-Co system: Martensitic transformation temperatures, assessment of gibbs energies and thermodynamic calculation of T0 lines, Le Journal de Physique IV 7 (C5) (1997) C5–405.
[47] S. Cotes, A. Baruj, M. Sade, A. Fernández Guillermet, Thermodynamics of the γ/ε martensitic transformation in Fe-Mn alloys: Modelling of the driving force, and calculation of the MS and AS temperatures,

Le Journal de Physique IV 5 (C2) (1995) C2–83.
[48] J. D. Honeycutt, H. C. Andersen, Molecular dynamics study of melting and freezing of small Lennard-Jones clusters, Journal of Physical Chemistry 91 (19) (1987) 4950–4963.
[49] M. Bixon, J. Jortner, Energetic and thermodynamic size effects in molecular clusters, The Journal of Chemical Physics 91 (3) (1989) 1631–1642.
[50] B. Vekhter, R. S. Berry, Phase coexistence in clusters: An experimental isobar and an elementary model, The Journal of Chemical Physics 106 (15) (1997) 6456–6459.
[51] S. Zamith, F. Chirot, J.-M. L'Hermite, A two-state model analysis of the melting of sodium clusters: Insights in the enthalpy-entropy compensation, EPL (Europhysics Letters) 92 (1) (2010) 13004.
[52] S. Foiles, J. Adams, Thermodynamic properties of fcc transition metals as calculated with the embedded-atom method, Physical Review B 40 (9) (1989) 5909.

Figure captions

Figure 1 Results of the MD simulations for Au nano-clusters with (a) N=1985, (b) N=15705 and (c) N=180313. First row: energy per atom (E/N) versus T relations ("caloric curves"). Second row: $\Delta(E/N)/\Delta T$ ratios. Third row: Lindemann index (Eq.(1)). Fourth row: $\Delta\delta_c/\Delta T$ ratios. The vertical dotted lines indicate the four stages of the melting transition (see text). The arrows with roman numbers indicate the onset of the "pre-melting" (I), as well as the onset (II) and the end (III) of the "melting step".

Figure 2 Section snapshot views of Au-clusters with N=1985 (2 nm), N=15705 (4 nm) and N=180313 (9 nm) at various temperatures upon heating. The vertical dotted lines indicate the same temperature ranges determined in Fig. 1. The atoms painted in red are those which were located at the surface layers at the onset of the heating process.

Figure 3 $RMSD$ of the atoms in spherical shells, referred to the interatomic distance $d = 2.9\dot{A}$ of Au as a function of the distance from the center of the cluster for various temperatures, for N=1985 (a), N=15705 (b) and N=180313 (c).

Figure 4 The effect of temperature upon the radius distribution function for the innermost ((a) and (c)) and outermost shells ((b) and (d)) in clusters with N=15705 ((a) and (b)) and N=180313 ((c) and (d)). The arrows are used to highlight some relevant differences between the patterns.

Figure 5 Energy and entropy of the "melting step" of nano-clusters with various numbers of atoms (N) as a function of $N^{1/3}$.

Figure 6 "Melting step" for a Au cluster with N=180313. The quantities involved in Eq.(8) are indicated

Figure 7 The effect of temperature upon the X_{SPL} (circles) and X_{LPL} (squares) variables obtained by applying Eqs. (8) and (9) to the MD results for nano-clusters with $N = 180313$ atoms. The vertical arrows in this plot indicate the temperature at which $K_{eq} = 1$.

Figure 8 Size dependence of the T_0 temperature, introduced in Section 4.3. Square symbols represent the results of the Eq.(6) and circle symbols those obtained by solving Eq. (14). Dashed lines represents the linear fit.

Figures

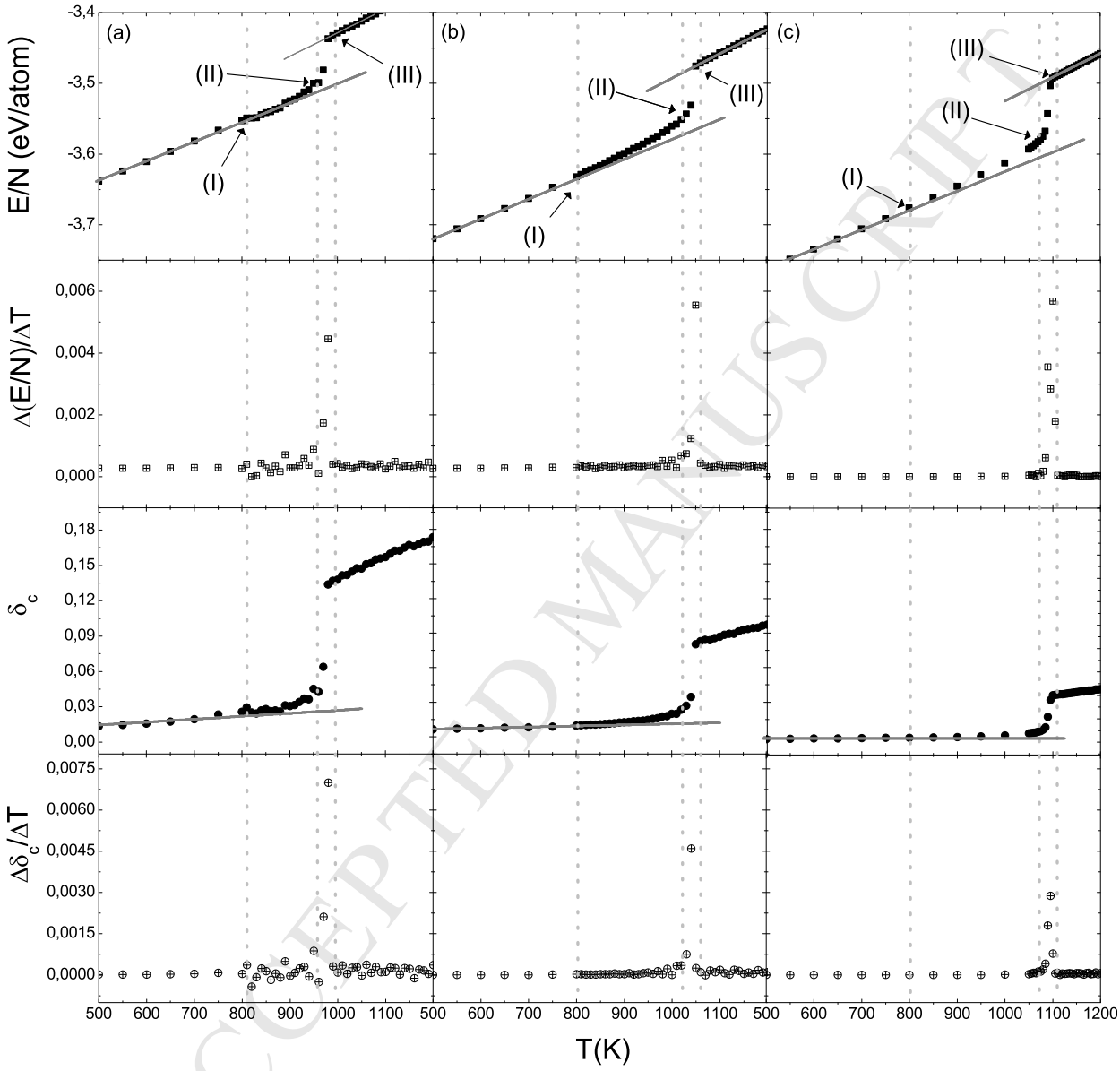

Figure 1:

Figure 2:

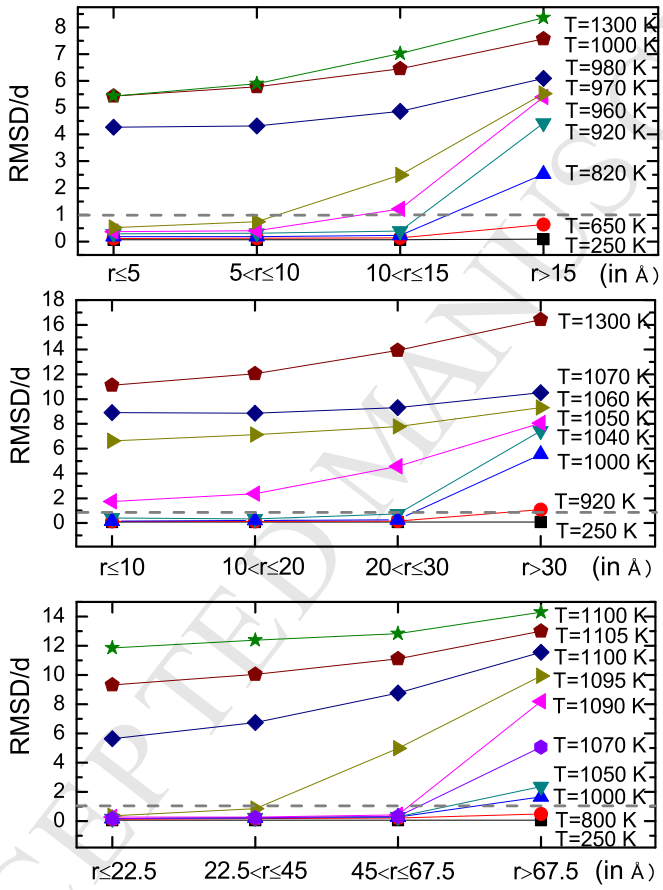

Figure 3:

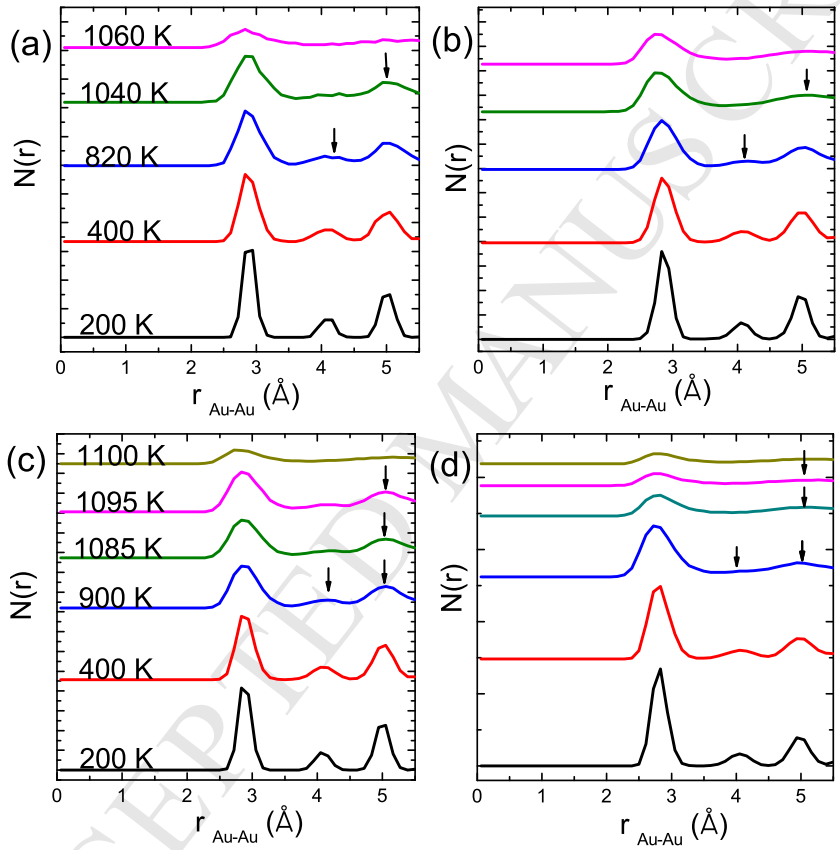

Figure 4:

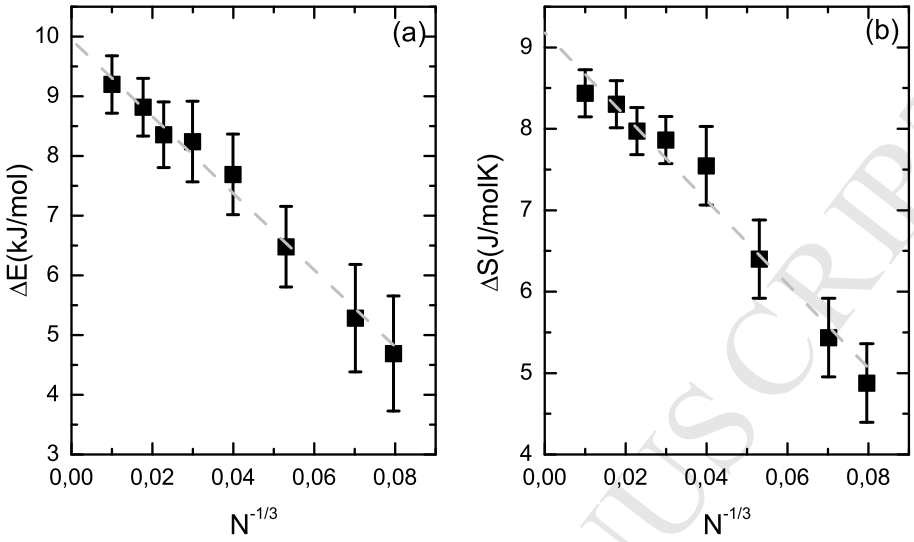

Figure 5:

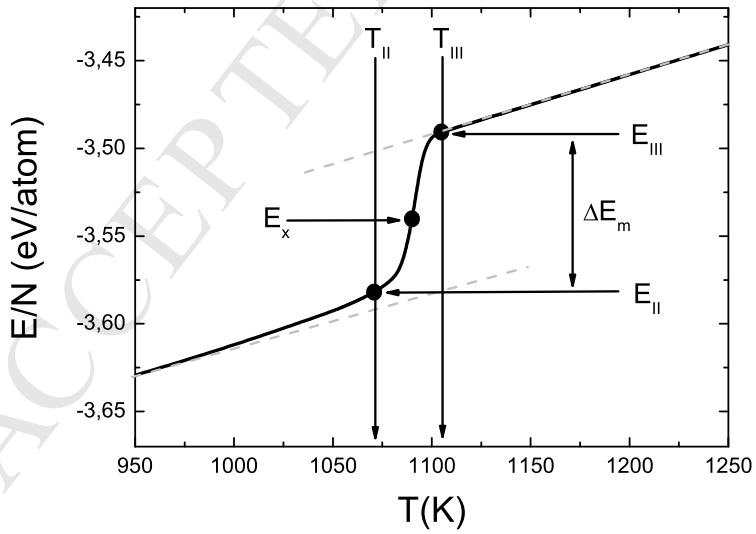

Figure 6: .

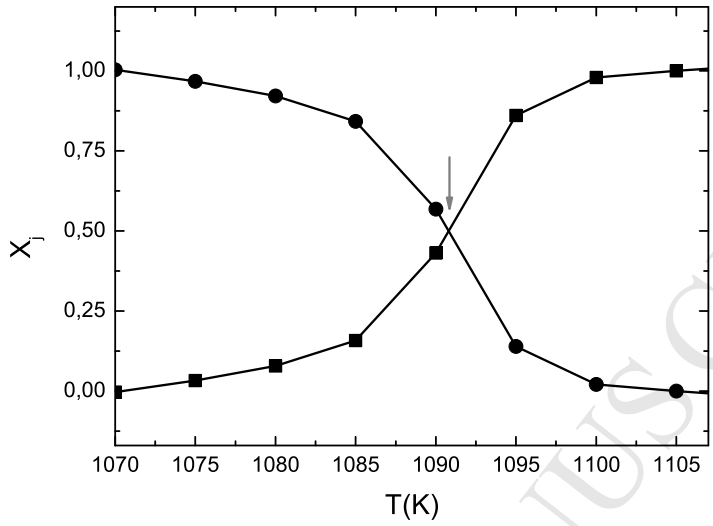

Figure 7:

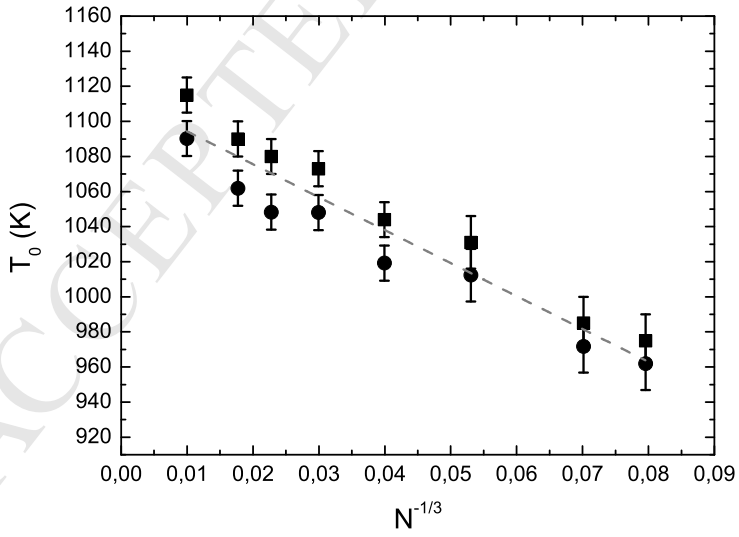

Figure 8: